Bulletin of Entomological Research

cambridge.org/ber

DNA barcoding-assisted classification of the genus *Actias* (Lepidoptera: Saturniidae)

Xin Fu, Su-Yang Bai, Long Chen, Chen Lv, Yu-Xuan He, Yu-Ping Li and Yan-Qun Liu

Department of Sericulture, College of Bioscience and Biotechnology, Shenyang Agricultural University, Shenyang, China

Research Paper

Cite this article: Fu X, Bai S-Y, Chen L, Lv C, He Y-X, Li Y-P, Liu Y-Q (2026) DNA barcoding-assisted classification of the genus *Actias* (Lepidoptera: Saturniidae). *Bulletin of Entomological Research* **116**, 478–494. https://doi.org/10.1017/S0007485326100893

Received: 29 May 2025
Revised: 3 January 2026
Accepted: 1 March 2026
First published online: 24 March 2026

Keywords:
Actias; DNA barcoding-assisted classification; genetic distance; geographic distribution; phylogenetic relationship

Corresponding author: Yan-Qun Liu;
Email: liuyanqun@syau.edu.cn

Abstract

The classification of the species in the genus *Actias* Leach, 1815 (Lepidoptera: Saturniidae) is challenging because many species have a highly similar morphology, while differences in database classification standards also provoke identification problems. To help resolve these issues, we conducted an integrative analysis of 741 cytochrome oxidase subunit I (COI) barcode sequences available by combining phylogenetic reconstruction, population genetic (Fst) metrics, and biogeographic data. This approach delineated 44 molecular operational taxonomic units (MOTUs) and established a genus-specific, empirical genetic distance threshold of 2.05% from a baseline of 29 morphologically validated MOTUs. These 29 MOTUs/morphospecies were then utilized to assess the interspecific genetic distance gap of this genus and further used as the species-level genetic distance to delimit the remaining morphospecies. Applying this multi-evidence framework allowed us to propose a significant re-evaluation of species boundaries, including several taxonomic reclassifications, and to generate the molecular inventory for *Actias*. Our study illustrates the power of an integrated molecular approach to resolve complex taxonomic issues and provides a robust, data-driven foundation for future research on *Actias*.

Introduction

Actias Leach, 1815 is a relatively small genus (the 'moon moths') of giant silk moths (Lepidoptera: Saturniidae) that comprises beautiful moths whose adults have long swallowtails on the hindwings (Nässig and Peigler, 1984; Hodges, 2005; Wu and Naumann, 2006; Zborowski and Edwards, 2007). This genus has been recorded in Asia, America, and Europe, and has potential significance in silk production (Collins and Weast, 1961), food consumption (Wagner, 2005), and as special pets due to the lovely and colourful larvae (Albertoni and Duarte, 2015).

The classification of *Actias* species is confusing and challenging because many species are morphologically highly similar. Hence, morphology-based species may be subject to a high risk of overlooking cryptic species (De Biaggi *et al.*, 2010; Ichter *et al.*, 2010). Consequently, the number of species in the genus *Actias* varies greatly, ranging from 41 to 46 (Ratnasingham and Hebert, 2007; Kitching *et al.*, 2018; Beccaloni *et al.*, 2024), and even up to 55 in Wikipedia (accessed on 4 March 2025). Although only two nuclear genomes (Triant and Pirro, 2023; Markee *et al.*, 2024) and six mitochondrial genomes of *Actias* species have been sequenced (Liu *et al.*, 2012; Park *et al.*, 2016; Zhao *et al.*, 2021; García-Souto *et al.*, 2025), there are many cytochrome oxidase subunit I (COI) sequences of *Actias* species available in the BOLD (https://portal.boldsystems.org/; Ratnasingham and Hebert, 2007) and NCBI databases (https://www.ncbi.nlm.nih.gov/) that may be helpful to establish the taxonomic classification of this genus.

For several decades, DNA sequence data have been used extensively to resolve taxonomic debates and test cryptic species. DNA barcoding based on COI sequences is an efficient tool to delineate taxa and link adult morphs with their developmental life stages in various insects (Hebert *et al.*, 2003; Alex Smith *et al.*, 2013; Tsai *et al.*, 2014). As such, DNA barcoding has also been used in the study of Lepidoptera species (e.g. Aguila *et al.*, 2012; Núñez *et al.*, 2020; Zhang *et al.*, 2021, 2022). More generally, by integrating phenotypic characteristics, geographic distribution, DNA barcodes, and phylogenetic analysis, a thorough classification approach has been proposed to re-examine classification problems (Sheth and Thaker, 2017).

To resolve taxonomic uncertainties within the genus *Actias*, we present in this study a global phylogenetic framework for this genus by integrating all available COI sequences from both the NCBI and BOLD databases. Building upon this foundation, we systematically evaluate species boundaries and establish a DNA data-driven, genus-specific genetic distance threshold to provide a more precise tool for species identification in the genus *Actias*. Furthermore, we seek to elucidate the phylogeographic patterns of *Actias* species by connecting phylogenetic relationships with geographical distributions, thereby offering new insights into the origin, dispersal, and speciation history of the genus.

© The Author(s), 2026. Published by Cambridge University Press.

Materials and methods

Research rationale and dataset assembly

This study was designed to establish a comprehensive global phylogenetic framework for the genus *Actias* in order to resolve several longstanding taxonomic uncertainties. Within this framework, we addressed specific taxonomic challenges in Liaoning Province, China, where the high morphological similarity between species complicates their identification. The overarching strategy was to construct a robust global reference dataset and then use it to validate existing public sequences from Liaoning and definitively identify newly collected specimens from Benxi, Liaoning Province.

To this end, all public COI sequences for the genus *Actias* were retrieved from the BOLD and NCBI databases (accessed on 4 March 2025) using the search strategy (e.g. '*Actias*' AND ('COI' OR 'cytochrome c oxidase subunit I')). Following a quality control pipeline (Schmidt *et al.*, 2015; Schattanek-Wiesmair *et al.*, 2024), the resulting curated public dataset was integrated with four new sequences from Benxi (generated for this study). This combined final dataset represents the global diversity of the genus and served as a reference for all subsequent phylogenetic and taxonomic analyses in this study (table S1).

Specimen collection and laboratory procedures

To assess the classification of *Actias* species from Liaoning Province, China, four adults of *Actias* specimens collected from Benxi, Liaoning Province, on 28 July 2023, were used (fig. S1). The femurs of the specimens were immersed in trace DNA extraction buffer (10 mmol/l Tris-HCl (pH 8.0), 10 mmol/l EDTA (pH 8.0), 100 mmol/l NaCl, 2% SDS, 0.039 mol/l DTT, and 100 mg/l proteinase K) (Wang *et al.*, 1997), incubated at 50°C for 2 h and then treated via the traditional phenol/chloroform method. A 658 base pair (bp) COI sequence was amplified using the primer set C1-J1483 (5'-GGTCAACAAATCATAAAGATATTGG-3') and C1-N2194 (5'-TAAACTTCAGGGTGACCAAAAAATCA-3') (Simon *et al.*, 2006). PCR amplification was conducted under the following conditions: initial denaturation at 90°C for 3 min, followed by 35 cycles at 90°C for 30 s, 55°C for 30 s, and a final extension at 72°C for 45 s. The PCR products were purified and directly sequenced with the PCR primers. Chromas 2.6.5 Software (Technelysium Pty Ltd, South Brisbane, Queensland, Australia) was used to read and confirm the sequencing read data. These four COI sequences were then used for species identification through DNA barcode analysis.

Preliminary data screening and alignment

Sequences retrieved from the BOLD and NCBI databases with lengths <500 bp were excluded for further analyses (Schmidt *et al.*, 2015; Schattanek-Wiesmair *et al.*, 2024). The dataset was deduplicated, with taxonomic precedence given to BOLD records in cases of conflict. Sequences that were confirmed to be non-COI fragments via MAFFT analysis were also removed (Katoh *et al.*, 2017). The remaining sequences were aligned using the MAFFT online service (https://mafft.cbrc.jp/alignment/server/) (Katoh *et al.*, 2017). This initial alignment was then used to construct a preliminary neighbour-joining (NJ) tree to screen for sequences that behaved as phylogenetic outliers (e.g. those exhibiting exceptionally long branches or unstable positions that distorted the tree topology). A minimal number of such outlier sequences were identified and excluded to ensure the robustness of the dataset for further analyses. The final, curated alignment was used for all subsequent analyses. MEGA 11 (Tamura *et al.*, 2021) was used to infer the numbers of invariable sites, polymorphic sites, parsimony informative sites, and singleton sites.

Species delimitation and K2P genetic distance analysis

To estimate the number of molecular operational taxonomic units (MOTUs), three methods were employed: Automatic Barcode Gap Discovery (ABGD), Assemble Species by Automatic Partitioning (ASAP), and Bayesian Poisson Tree Processes (bPTP). The ABGD analysis was conducted online (https://bioinfo.mnhn.fr/abi/public/abgd/abgdweb.html) with the default settings, using a relative gap width ($X = 1.1$) and intraspecific divergence (P) values between 0.001 and 0.1 with the Kimura-2-Parameter (K2P) model (Puillandre *et al.*, 2012). The ASAP analysis was performed using a web browser (https://bioinfo.mnhn.fr/abi/public/asap/) with the Jukes–Cantor (JC69) model and default settings (Puillandre *et al.*, 2021). The bPTP analysis was run on the web server (http://species.h-its.org/ptp) with 100,000 Markov Chain Monte Carlo Method (MCMC) generations and default parameters (Zhang *et al.*, 2013). Intra- and interspecific K2P distances among *Actias* COI sequences were calculated using MEGA 11 (Tamura *et al.*, 2021).

To quantify the genetic differentiation between evolutionarily ambiguous lineages identified in our global phylogenetic tree, we computed Fst values. These 'populations' for Fst analysis were defined as specific MOTUs or subclades with ambiguous taxonomic status (e.g. allopatric lineages with shallow genetic divergence, or parapatric lineages with deep splits) derived from the global dataset. Fst values between populations with ambiguous taxonomic status were computed using DnaSP 6 (Rozas *et al.*, 2017) and Arlequin suite v. 3.5 (Excoffier and Lischer, 2010).

Geographic phylogeny

An NJ tree was constructed with MEGA 11 (Tamura *et al.*, 2021), with the following settings: bootstrap method (1000 replications), model (maximum composite likelihood), substitutions (transitions + transversions), and missing data treatment (pairwise deletion). The Chinese oak silkmoth (Saturniidae) *Antheraea pernyi* (Guérin-Méneville, 1855) (GenBank ID: OQ272864) and the domestic silkmoth (Bombycidae) *Bombyx mori* (Linnaeus, 1758) (GenBank ID: JF700137) were used as outgroup taxa. ArcMap 10.8.1 (ESRI, 2020) was used to map the geographic location of the COI sequences of *Actias* species, according to the geographic information retrieved from the BOLD database (table S2).

Results

Sequence information

The final dataset of 741 COI sequences from the genus *Actias* was assembled for analysis. This was achieved by merging an initial set of 848 public sequences from BOLD (736) and NCBI (112), which involved removing 105 duplicate records (prioritizing BOLD taxonomy) and 6 problematic sequences (4 non-COI (KT026042, KX302402, SATWG001-18, and GBGLS178-19; fig. S2), and 2 short outliers (SAUPA121-09 and SAUPA122-09; fig. S3)), resulting in 737 curated public sequences (table S1) (Pu *et al.*, 2008; Hebert *et al.*, 2010; Zhong, 2016; García-Souto

https://doi.org/10.1017/S0007485326100893 Published online by Cambridge University Press

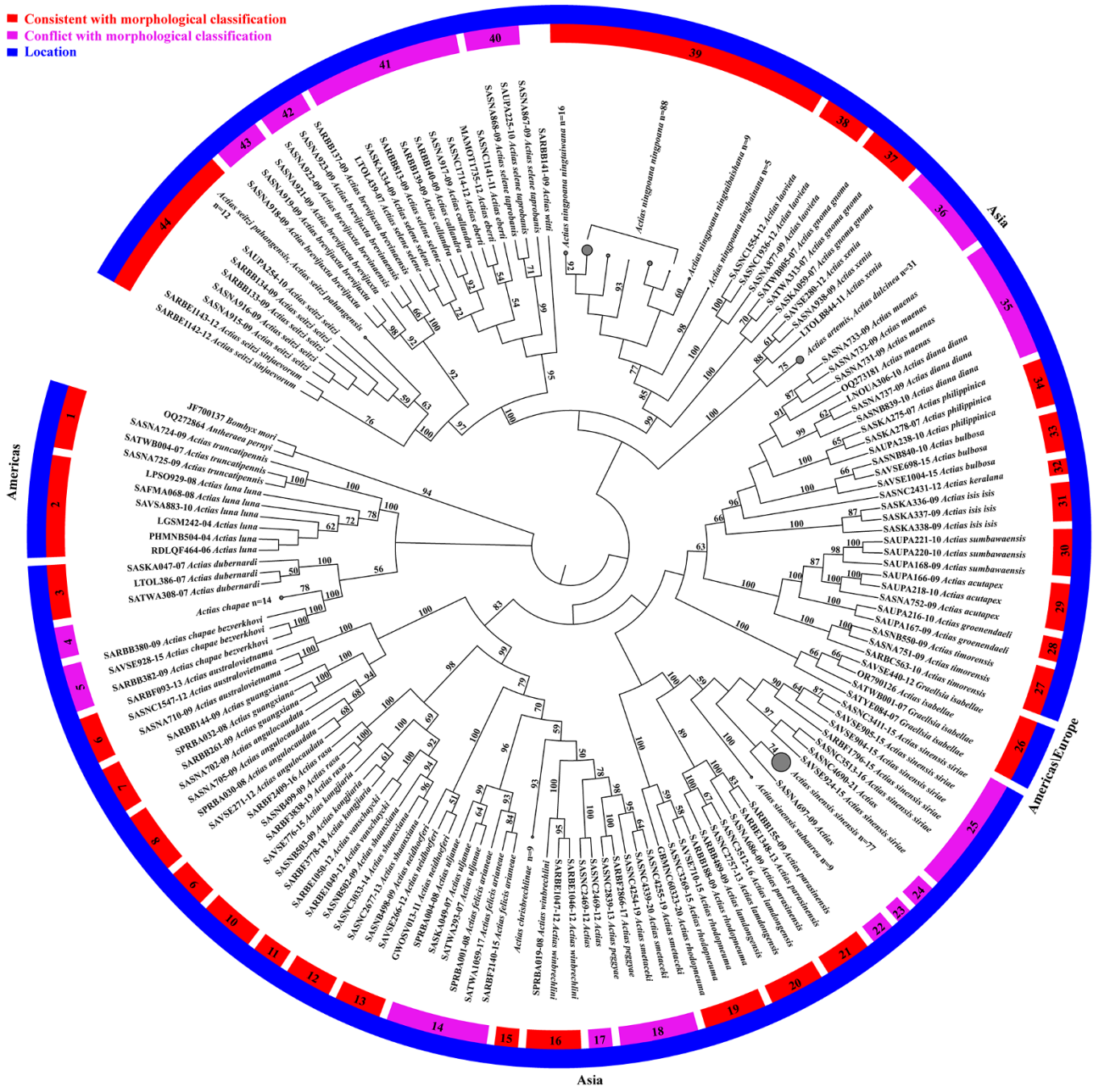


Figure 1. Phylogenetic relationships of 44 MOTUs based on COI sequences of the genus *Actias* inferred by neighbour-joining of K2P distances. Red blocks, MOTUs that are consistent with morphological classification; purple blocks, MOTUs that are in conflict with morphological classification; and blue blocks, geographic areas. For 29 MOTUs that agree well with morphological classification, 1–3 representative sequences are selected for each species. Numbers 1–44 indicate the numbering of MOTUs; *n* = sample size.

et al., 2025). These were combined with the four new sequences (PV628723, PV628724, PV628729, and PV628734; fig. S1) from Benxi, Liaoning Province (this study) to form the final dataset representing 46 morphospecies (table S2).

A total of 707 sequences with length >600 bp were selected for sequence comparison. In the alignment of 658 bp, there were 403 invariable sites (61.25%), 227 parsimony informative sites (34.50%), 28 singleton sites (4.25%), and 255 polymorphic sites (38.75%).

DNA barcoding-based species delimitation of the genus Actias

While ABGD and ASAP yielded largely congruent and stable results, the bPTP analysis produced inconsistent and poorly supported groupings that conflicted with both the morphological evidence and the phylogenetic structure. Similar instabilities with bPTP analysis have been reported in other lepidopteran groups (Tsai *et al.*, 2014; Guo *et al.*, 2024; Schattanek-Wiesmair *et al.*, 2024). Therefore, we did not rely on the bPTP results, but based our final MOTU delineation on the consensus of ABGD,

https://doi.org/10.1017/S0007485326100893 Published online by Cambridge University Press

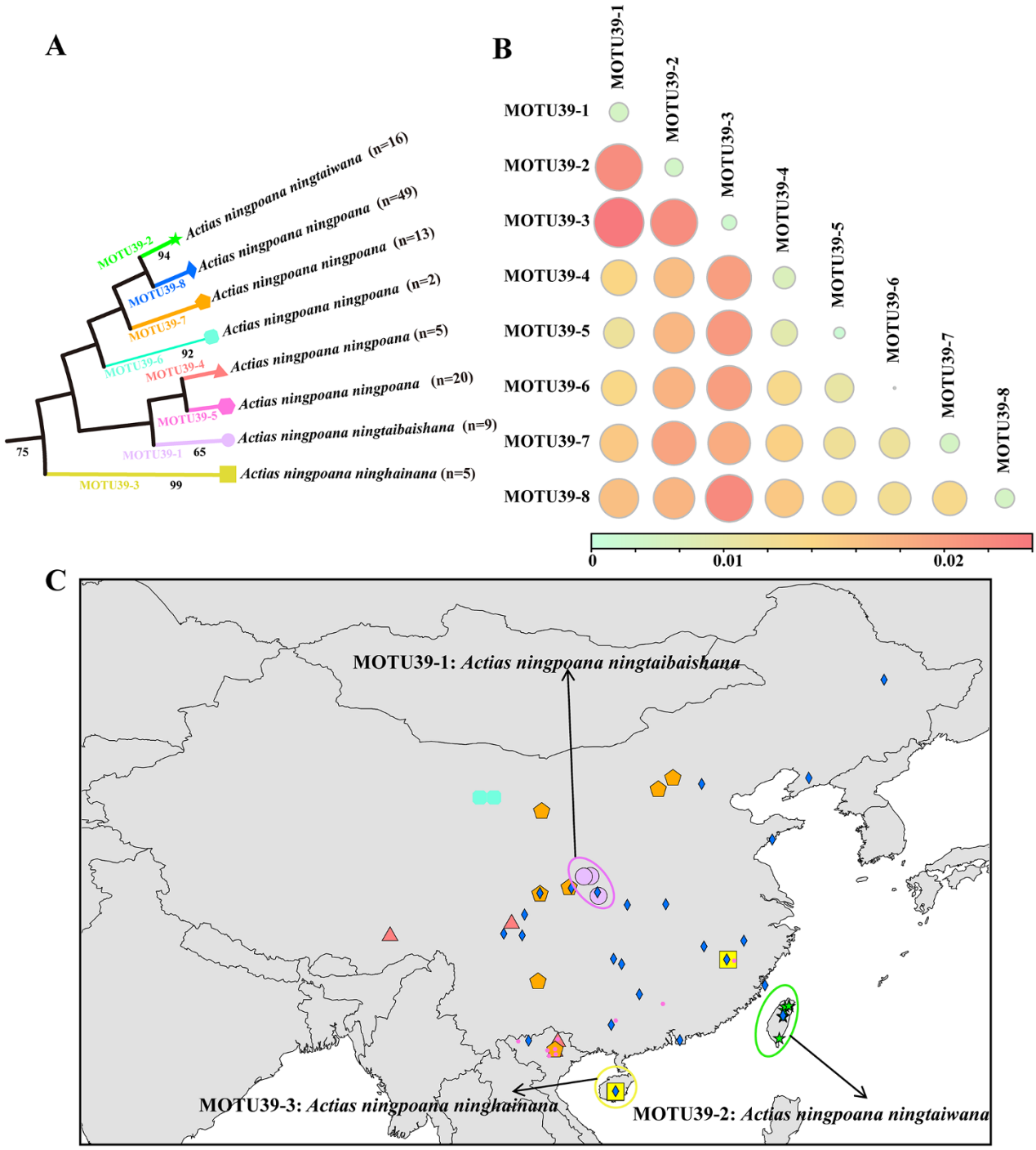


Figure 2. Neighbour-joining tree (A), K2P COI distance (B), and geographical distribution (C) of potential subspecies in MOTU39 (*A. ningpoana*).

ASAP, phylogenetic monophyly, and genetic distances. Using this comprehensive dataset, we delineated 44 MOTUs for the genus *Actias* (fig. 1, table S2). Of these, 29 MOTUs showed complete concordance with well-established morphospecies and formed distinct, well-supported clades (bootstrap > 77%) (fig. 1, table S3). We used this set of 29 robust and consistent taxa as a baseline to estimate the first genus-specific genetic distance threshold for *Actias* species. The full range of interspecific K2P COI distances within this baseline dataset was 2.05–14.56% (table S3). We therefore defined this minimal value (2.05%) as the empirical COI-sequence-based genetic distance threshold for species delimitation in the genus. This threshold was subsequently applied to evaluate the taxonomic status of the remaining MOTUs that conflicted with initial morphological classifications, helping to identify potential cryptic diversity or misidentifications in relation to our proposed classification for *Actias* as summarized in table S4.

https://doi.org/10.1017/S0007485326100893 Published online by Cambridge University Press

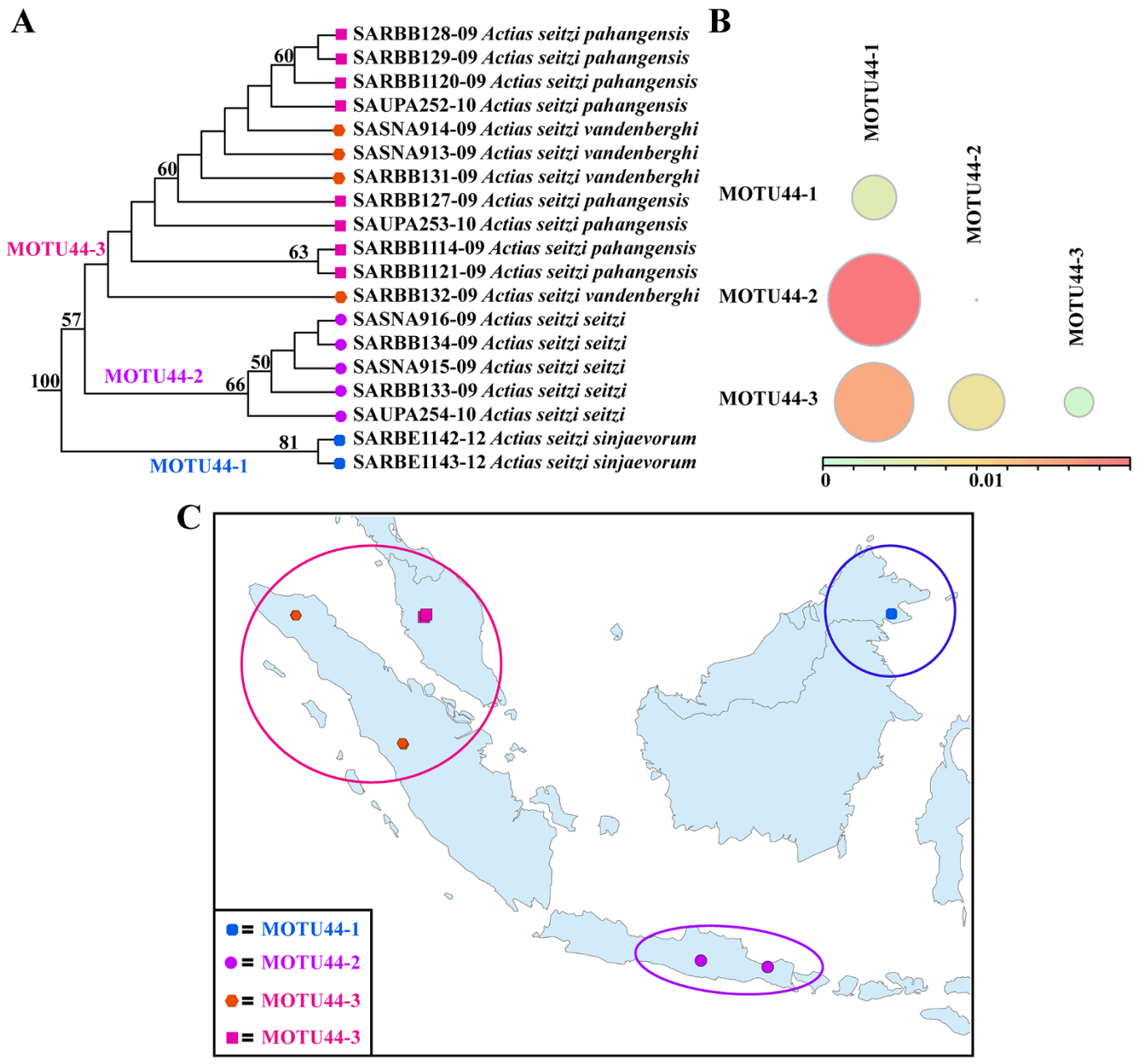


Figure 3. Neighbour-joining tree (A), K2P COI distance (B), and geographical distribution (C) of one species and three subspecies in MOTU44 (*A. seitzi*).

DNA barcoding-based assessment of subspecies delimitation in the genus Actias

To establish a reference for subspecific genetic distances within the genus *Actias*, we analysed three morphologically well-defined lineages of *Actias ningpoana* Fielder, 1862 viz. *A. n. ningtaibaishana* Brechlin, 2013 (MOTU39-1), *A. n. ningtaiwana* Brechlin, 2012 (MOTU39-2), and *A. n. ninghainana* Brechlin, 2012 (MOTU39-3). These lineages show very low intrasubspecific K2P COI distances (0.18–0.40%) (fig. 2), consistent with typical intraspecific variation. Yet, the intersubspecific K2P COI distances between them (1.79–2.03%) exhibited a characteristic 'intermediate state'. They were substantially greater than routine intraspecific divergence (>1%), though they remained below the *Actias*-specific interspecific threshold of 2.05% established in this study. This empirical range for intersubspecific COI divergences provides another quantitative baseline to help interpreting COI genetic distances in *Actias*.

Accordingly, we define a practical operational criterion for subspecific distinction in *Actias* as a K2P COI distance range of >1.00% to <2.05%. This criterion was applied to evaluate other potential subspecies within the genus. Furthermore, in line with the logic of Núñez *et al.* (2023), we interpret any lineage that is separated by a barcode gap exceeding 2.05% from its nearest conspecific population as having reached species-level distinction.

https://doi.org/10.1017/S0007485326100893 Published online by Cambridge University Press

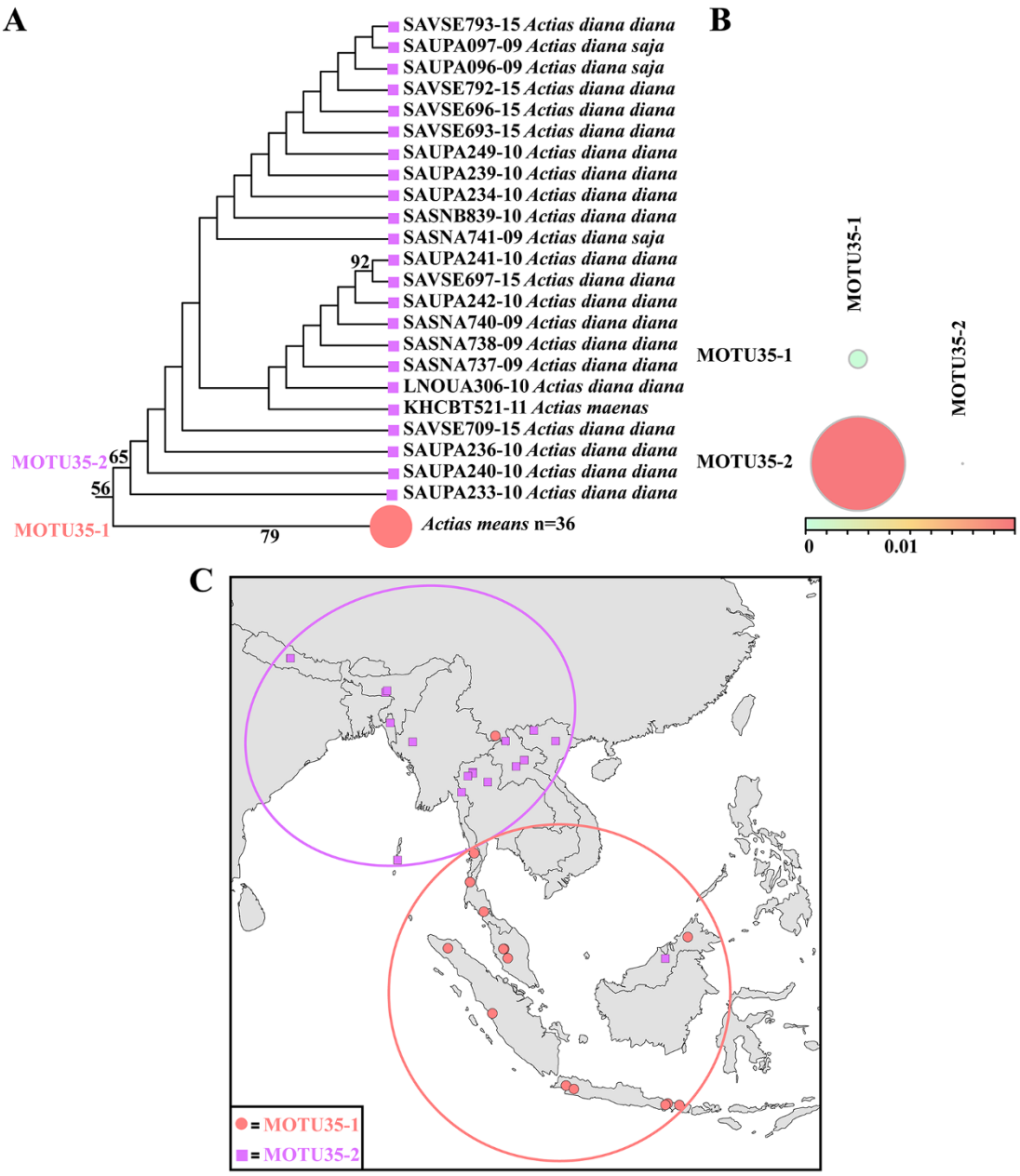


Figure 4. Neighbour-joining tree (A), K2P COI distance (B), and geographical distribution (C) of one species and two subspecies in MOTU35 (*A. maenas* and *A. diana*).

Assessment of infraspecific diversity and potential subspecies

Following the clarification of species boundaries, we investigated complex internal genetic structures within several MOTUs to assess infraspecific diversity. Our analysis integrated the genus-specific K2P COI distance criterion (1.00–2.05%) with phylogenetic, geographical, and population genetic (Fst) evidence to evaluate putative subspecies boundaries.

Within *A. ningpoana* (MOTU39), the nominal subspecies *A. n. ningpoana* (89 specimens) comprised 5 distinct subclades (fig. 2A). These subclades exhibited significant COI differentiation (Fst = 0.35–0.91) (table S5), with K2P COI distances in the range 0.56–1.19% (fig. 2B, C), falling within the subspecific threshold range, despite their largely sympatric distribution. Given this substantial differentiation that exceeds typical intraspecific variation, but that does not warrant species-level distinction, we interpret these as well-differentiated infraspecific subclades, the taxonomic status of which awaits clarification by incorporating more integrative data in future study.

Conversely, the case of *Actias seitzi* Kalis, 1934 (MOTU44) provided a compelling, three-tiered demonstration of how our framework resolved complex infraspecific taxonomy by integrating multiple lines of evidence. Phylogenetic analysis grouped the morphologically defined *A. s. pahangensis* Brechlin, 2012 and *A. s. vandenberghi* (GBIF Secretariat, 2023) into a single, mixed subclade (MOTU44-3). This consolidation was strongly supported by their mean K2P COI distance of 0.17% (fig. 3), adjacent geographical distributions, and a negligible population genetic differentiation (Fst = 0.102) (table S6). Collectively, this suggests that

https://doi.org/10.1017/S0007485326100893 Published online by Cambridge University Press

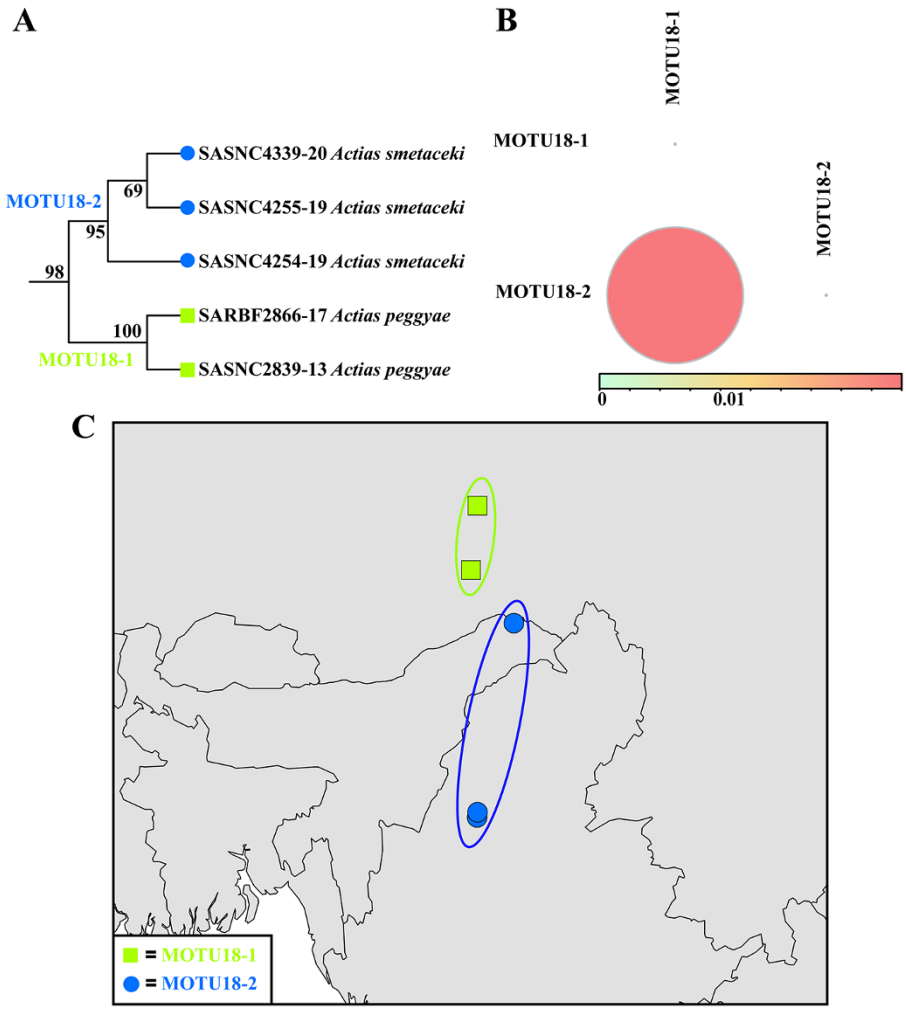


Figure 5. Neighbour-joining tree (A), K2P COI distance (B), and geographical distribution (C) of one species and two subspecies in MOTU18 (*A. smetaceki* and *A. peggyae*).

they represent a single interbreeding population and thus are better interpreted as a single subspecies. We therefore propose the synonymization of these two subspecific names. The case of *A. s. sinjaevorum* Brechlin, 2012 (MOTU44-1) provides an intermediate scenario. Its mean K2P COI distances to the other subclades (0.83% and 1.11%) approached or fall within the lower bound of the proposed subspecific threshold. This, together with its clearly allopatric distribution, provides compelling evidence for its recognition as a distinct subspecies. Finally, the distinction between the consolidated MOTU44-3 and *A. s. seitzi* (MOTU44-2) was critically supported by population genetic evidence (fig. 3C). Despite a mean intersubspecific K2P COI distance (0.44%), their allopatric distributions and a high pairwise Fst value (> 0.76) (table S6) suggest a pronounced lack of gene flow and substantial genetic differentiation, robustly supporting their status as distinct subspecies. Thus, across a spectrum of genetic divergence, the integration of phylogenetic, genetic, and geographic evidence robustly supported the recognition of three, rather than four, valid subspecies within the *A. seitzi* complex.

Re-assessment of species boundaries: evidence for consolidation and division

Equipped with the empirically derived species (2.05%) and subspecies (1.00–2.05%) COI divergence thresholds, we next applied this two-tiered framework to systematically re-evaluate the taxonomic status of the 15 MOTUs that conflicted with prior morphological classifications.

The taxonomic relationship between *Actias maenas* (Doubleday, 1847) (MOTU35-1, $n = 36$) and *A. diana* Maassen, 1872 (MOTU35-2, $n = 22$) has been historically unstable. Our COI data reveal that both entities form a well-supported clade with a maximal K2P COI distance of 1.54% between specimens (fig. 4), which falls within the *Actias*-specific subspecific threshold range (1.00–2.05%). Their largely allopatric distributions, with minimal range overlap, provide additional evidence for a subspecific interpretation, in line with the historical treatment of *A. diana* as a subspecies of *A. maenas*. The integrated evidence hence supports the subspecific classification of *A. diana* (as *A. maenas diana*). Regarding the infraspecific structure within '*A. diana*' (MOTU35-2), the available sequences ($n = 22$) of two subspecies *A. d. diana* and *A. d. saja* were intermingled in the phylogeny and exhibited minimal COI divergences (0.15–0.45%), consistent with population-level variation rather than subspecific differentiation. Therefore, we do not uphold this subspecific division of MOTU35-2.

Similarly, MOTU18 contained sequences of both *Actias peggyae* Brechlin, 2017 ($n = 2$) and *A. smetaceki* Naumann, 2023 ($n = 3$). The maximal K2P COI distance of 1.36% between them fell within the subspecific threshold (fig. 5), and their distributions

https://doi.org/10.1017/S0007485326100893 Published online by Cambridge University Press

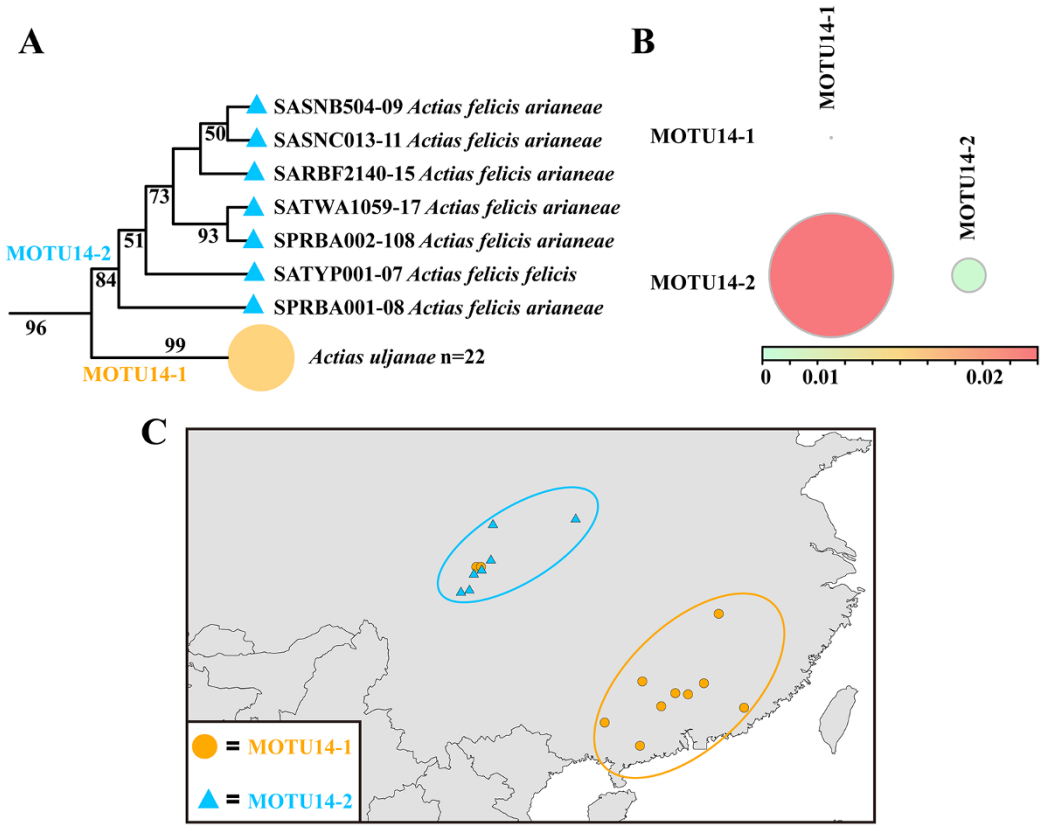


Figure 6. Neighbour-joining tree (A), K2P COI distance (B), and geographical distribution (C) of potential subspecies in MOTU14 (*A. felicis* and *A. uljanae*).

were largely allopatric. Following the rationale applied for *A. diana* and *A. maenas*, the evidence supported treating *A. smetaceki* as a subspecies of *A. peggyae*.

The same rationale was also applied to *Actias felicis* (Oberthür, 1896) and *A. uljanae* Brechlin, 2007, two distinct, but monophyletic, morphospecies (see for *A. felicis* MOTU14-2 ($n = 7$) and for *A. uljanae* MOTU14-1 ($n = 22$) in fig. 6A). However, they are separated by a mean K2P COI distance of 1.83%, which is in the 1.00–2.05% range, suggesting that they might be interpreted as subspecies of the same species (fig. 6B). Their largely allopatric distributions (fig. 6C) further support the subspecific relationship. This reclassification applies to the relationship between *A. uljanae* and the *A. felicis* complex as a whole. Within the *A. felicis* complex, the low K2P COI distances (0.76–0.92%) between the single sequence of the nominal subspecies *A. f. felicis* and all sequences of *A. f. arianeae* Brechlin, 2007 support their current status as conspecific. A definitive assessment of the subspecific boundary between *A. f. felicis* and *A. f. arianeae*, however, requires a larger sample size for the nominal subspecies and remains a focus for future research.

Based on morphology, 10 of the *Actias* specimens were recognized as representing 2 subspecies of *A. brevijuxta* Nässig & Treadaway, 1997, viz. *A. b. brevijuxta* and *A. b. brevinaensis* Brechlin, 2012. Our DNA barcoding analysis grouped these specimens into two well-supported MOTUs (MOTU42 and MOTU43; fig. 7), separated by a mean K2P COI distance of 2.19%, which exceeds the species-level threshold for the genus *Actias*. These two MOTUs also have largely allopatric distributions with only a minor zone of sympatry. Hence, the COI and biogeographical evidences support their recognition as distinct species.

Delineation of infraspecific diversity: assessment of subspecific boundaries

Phylogenetic analysis of 15 COI sequences of *Actias chrisbrechlinae* Brechlin, 2007 (MOTU15) yielded 3 well-supported subclades (fig. 8A). The mean K2P COI distance between these subclades was 1.55%, falling within the *Actias*-specific subspecific threshold range (fig. 8B). The three subclades also have large allopatric distributions (fig. 8C). Together, these evidences indicate that *A. chrisbrechlinae* comprises three well-differentiated, geographically structured infraspecific lineages. Formal description of these as subspecies, however, would require confirmation through an integrated morphological study.

Resolution of complex taxonomic scenarios involving multiple levels

Actias artemis (Bremer & Grey, 1853), *A. dulcinea* (Butler, 1881), and *A. xenia* (Jordan, 1912) are three distinct morphospecies. Yet, DNA barcoding-based phylogenetic analysis showed that *A. artemis* ($n = 8$) and *A. dulcinea* ($n = 12$) form a mixed clade, suggesting that they may be conspecific. Moreover, although *A. dulcinea*/*A. artemis* (MOTU36-2, $n = 20$) and *A. xenia* (MOTU36-1, $n = 9$) form two clades (fig. 9A), their maximal K2P COI distance of 1.38% (fig. 9B) is in the 1.00–2.05% range, suggesting that they might be interpreted as subspecies. This interpretation is also supported by the largely disjunct distribution, with *A. xenia* primarily found in Japan and *A. dulcinea*/*A. artemis* in the neighbouring regions of China, North Korea, South Korea, and Russia (fig. 9C).

https://doi.org/10.1017/S0007485326100893 Published online by Cambridge University Press

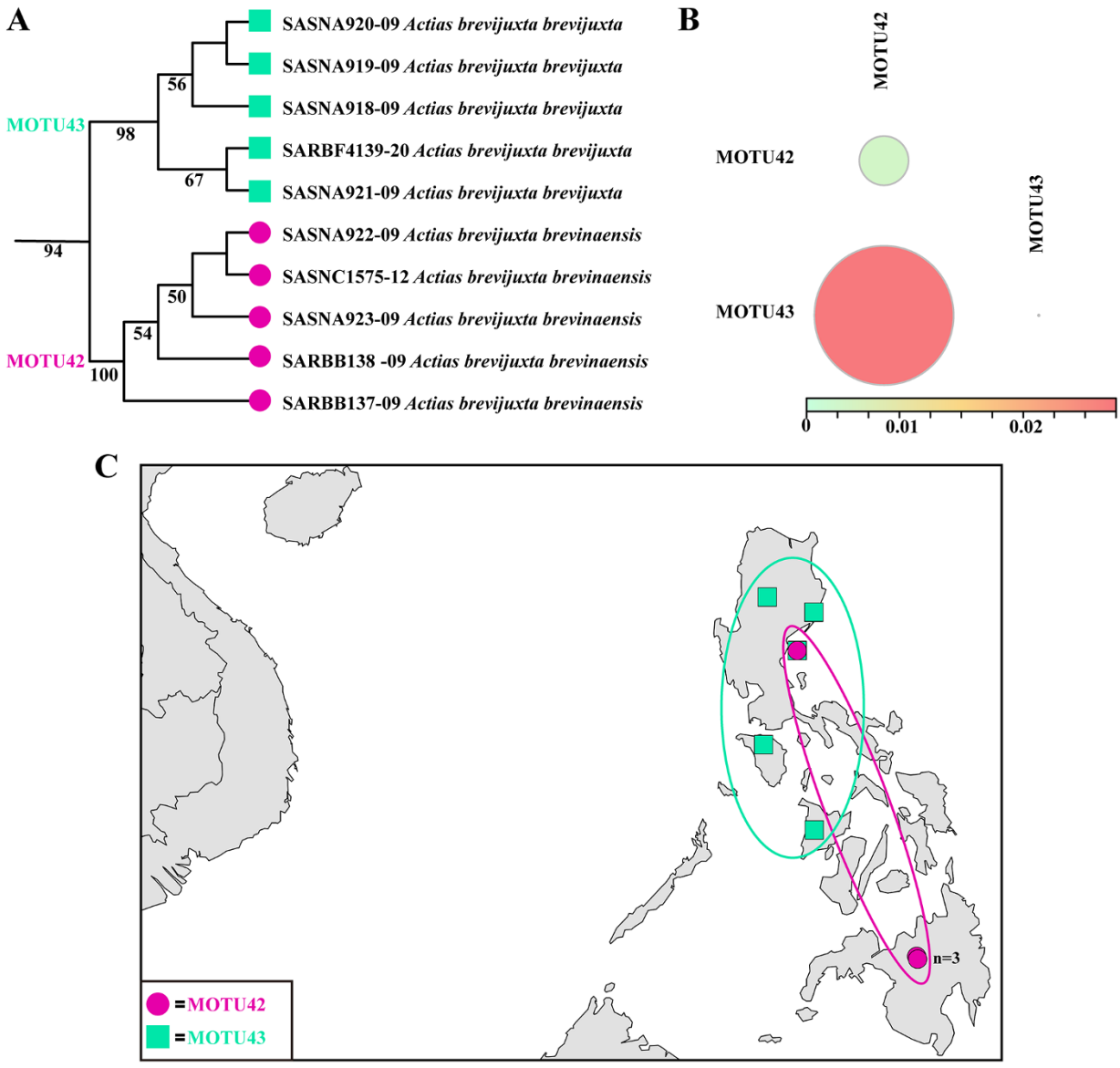


Figure 7. Neighbour-joining tree (A), K2P COI distance (B), and geographical distribution (C) of two species in MOTU42 and MOTU43 (*A. brevijuxta*).

Hence, this combined evidence suggests that these two clades are conspecific and may represent two subspecies.

Actias selene (Hübner, 1807) is a widely distributed species in southern Asia. Phylogenetic analysis grouped *A. selene* ($n = 40$) into MOTU40 and MOTU41. MOTU40 contained 8 sequences of *A. s. taprobanis* Paukstadt & Paukstadt, 1999, and MOTU41 included 31 sequences of *A. s. selene* (MOTU41-1), 3 sequences of *A. callandra* Jordan, 1911 (MOTU41-2), and 40 sequences of *A. eberti* Rougeot, 1969 (MOTU41-3) (fig. 10A). The mean K2P COI distance between MOTU40 and MOTU41 was 2.15% (fig. 10B), which exceeds the species-level threshold. Moreover, these two MOTUs have widely separated distributions (fig. 10C). These combined evidences support their species-level distinction. Moreover, MOTU41-1 (*A. s. selene*), MOTU41-2 (*A. callandra*), and MOTU41-3 (*A. eberti*) are separated by a K2P COI distance range of 1.14–1.39%, falling within the subspecific threshold range. These three MOTU41s also have allopatric distributions, further suggesting their subspecific variations. This structure conflicts with the current classification of *A. s. taprobanis* (MOTU40) and *A. s. selene* (MOTU41-1) as conspecifics, while supporting the inclusion of *A. callandra* (MOTU41-2) and *A. eberti* (MOTU41-3) within the *A. selene* (sensu stricto) species complex as subspecies.

Actias sinensis (Walker, 1855) is a widely distributed species in Asia that comprises three morphological subspecies: *A. s. sinensis, A. s. siriae* Brechlin & van Schayck, 2017, and *A. s. subaurea* Kishida, 1993. DNA barcoding-based phylogenetic analysis divided *A. sinensis* into MOTU22-25 (fig. 11A). These four MOTUs showed K2P COI distances of 2.22–4.23% (fig. 11B), i.e. >2.05% and thus suggested a species-level separation. This COI evidence, coupled with their allopatric distributions (fig. 11C), supports their interpretation as distinct species. The unique sequence SASNA697-09 (MOTU23, from Thailand) exhibits a 2.65% minimal K2P genetic distance from MOTU24, providing preliminary molecular evidence for its distinct taxonomic status. Here it is designated as a potential new lineage requiring future verification. However,

https://doi.org/10.1017/S0007485326100893 Published online by Cambridge University Press

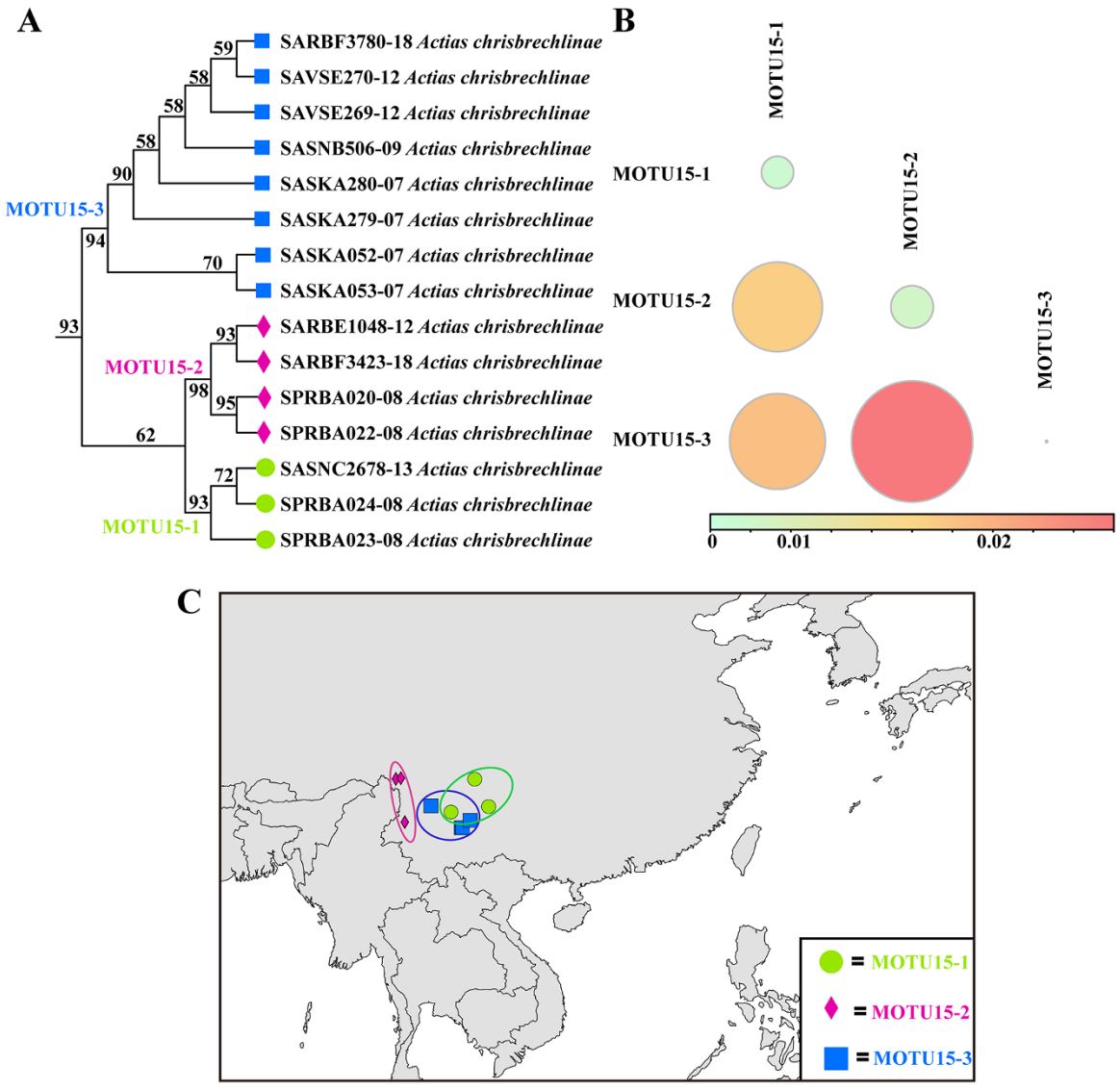


Figure 8. Neighbour-joining tree (A), K2P COI distance (B), and geographical distribution (C) of potential subspecies in MOTU15 (*A. chrisbrechlinae*).

evidence based on a single specimen is insufficient to draw a definitive conclusion. In this complex, the sequence of *Actias heterogyna* Mell, 1914 was embedded within MOTU24 and has a mean K2P COI distance of less than 1.00% from all *A. s. sinensis* sequences ($n = 76$), supporting a potential synonymization. Furthermore, the six individuals of the morphological subspecies *A. s. siriae* were grouped into two subclades (MOTU25-1 and MOTU25-2; fig. 11A), separated by a mean K2P COI distance of 1.91%. The various MOTUs show largely parapatric distributions: MOTU25-1 occurs in southeastern Vietnam (14.63°N), while MOTU25-2 is primarily distributed in northwestern Vietnam (16.52°N). Although one sampling site (15.99°N) contained individuals from both these MOTUs, the overall pattern of geographic separation supports the hypothesis of limited gene flow, which is consistent with their treatment as distinct subspecies.

Actias chapae Mell, 1950 comprises two subspecies, *A. c. chapae* and *A. c. bezverkhovi* Sochivko & Ivshin, 2008. DNA barcoding-based phylogenetic analysis resolved these two morphological subspecies into two clades (MOTU4 and MOTU5, respectively; fig. 12A). The mean K2P COI distance between them was 2.33% (fig. 12B), which exceeds the species-level threshold. This supports their recognition as distinct species. Within MOTU4 (*A. c. chapae*), the sequences were further grouped into four subclades. The K2P COI distances between these subclades fell within the range of 1.00–2.05%, supporting their interpretation as distinct subspecies. The allopatric distributions of *A. c. bezverkhovi* and the four subspecies in MOTU4 provide complementary evidence for this classification (fig. 12C).

For *Actias witti* Brechlin, 2007, only a 506 bp COI sequence was available. Its phylogenetic position varied during the construction of the phylogenetic tree, indicating that its taxonomic status needs to be addressed in the future. This principle, whereby infra-specific taxa that lack phylogenetic support within a MOTU are not recognized, also applies to other species in our study, such as *Actias luna* ($n = 45$), *A. diana* ($n = 22$), *A. maenas* ($n = 35$), *A. felicis* ($n = 7$), *Actias isis* Sonthonnax, 1897 ($n = 11$), and *A. artemis* ($n = 8$). For these and other cases listed in table S4, our COI data do not support the recognition of the described subspecies mentioned,

https://doi.org/10.1017/S0007485326100893 Published online by Cambridge University Press

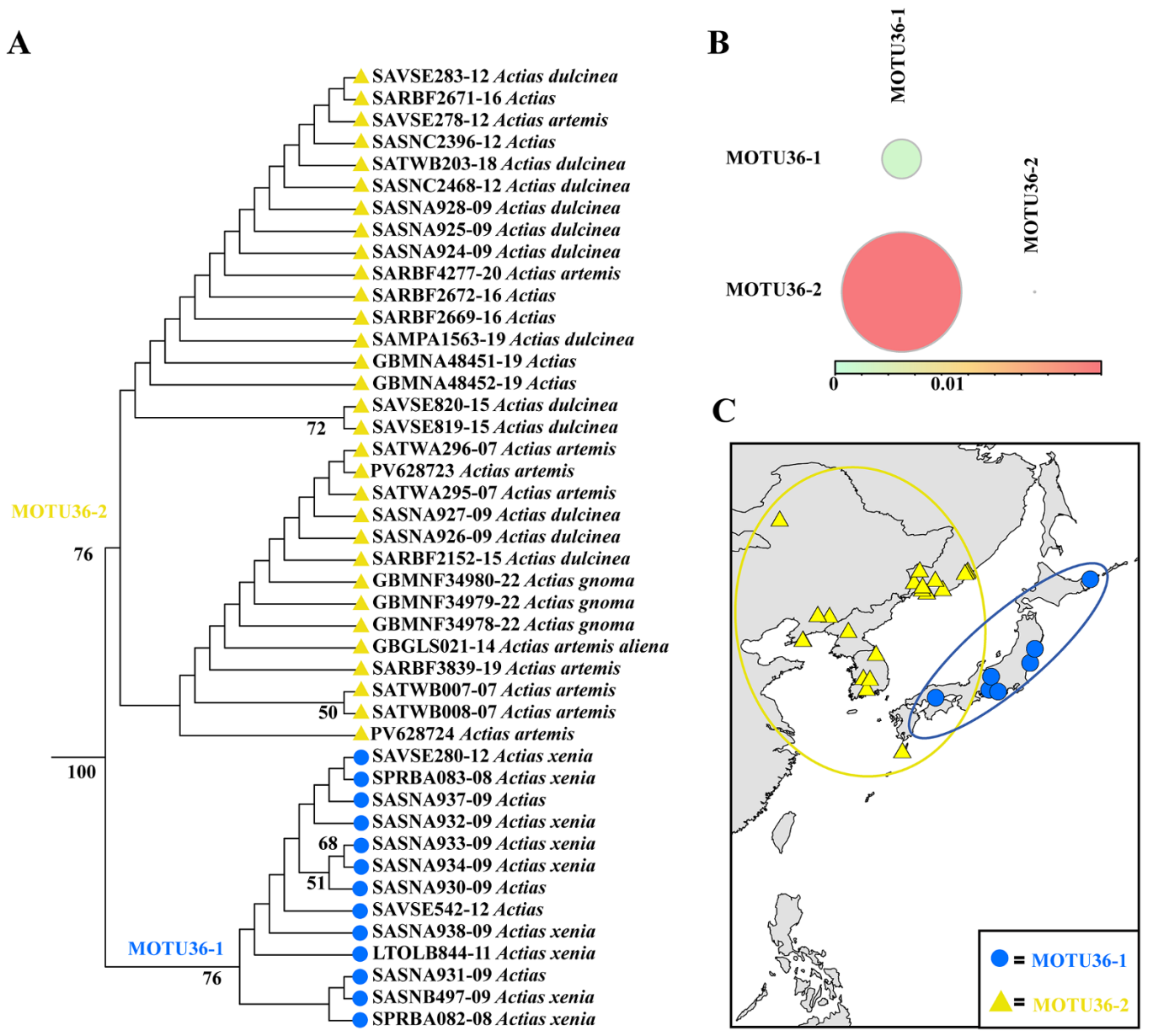


Figure 9. Neighbour-joining tree (A), K2P COI distance (B), and geographical distribution (C) of potential subspecies in MOTU36 (*A. artemis, A. dulcinea*, and *A. xenia*).

and we therefore treat these MOTUs as taxonomic units without subspecific division.

Phylogenetic placement of extra-limital species

Our comprehensive dataset allowed us to critically evaluate the taxonomic placement and COI differentiation of several historically challenging, extra-limital species. For the Spanish moon moth, *Actias* (*Graellsia*) *isabellae* (Graells, 1849), our analysis of 24 COI sequences retrieved from BOLD showed interspecific K2P COI distances to other *Actias* species ranging from 9.54% to 12.52%, well within the *Actias*-specific interspecific range (2.05–14.56%) observed across our study. Phylogenetically, *A. isabellae* was robustly placed within a clade comprising exclusively Asian *Actias* species, including *A. maenas* and *A. timorensis* (fig. 1). This close phylogenetic relationship stands in contrast to its allopatric distribution in Europe. For the American moon moths, *A. luna* (Linnaeus, 1758) ($n = 45$) and *A. truncatipennis* (Sonthonnax, 1899) ($n = 9$), the analysis of COI sequences confirmed their status as distinct species. Their K2P COI distances to Asian congeners also fell within the typical *Actias*-specific interspecific range. Crucially, phylogenetic analysis grouped them within a well-supported clade of Asian species, specifically as a sister taxon to a lineage containing *A. dubernardi* and *A. chapae* (fig. 1).

Assessment of sequence identifications in public databases

The comprehensive phylogenetic framework established in this study enabled a critical assessment of taxonomic assignments in public databases, leading to the re-identification of 13 sequences out of 741 used sequences. In the COI-based phylogenetic framework, these 13 sequences were deeply embedded within a MOTU

https://doi.org/10.1017/S0007485326100893 Published online by Cambridge University Press

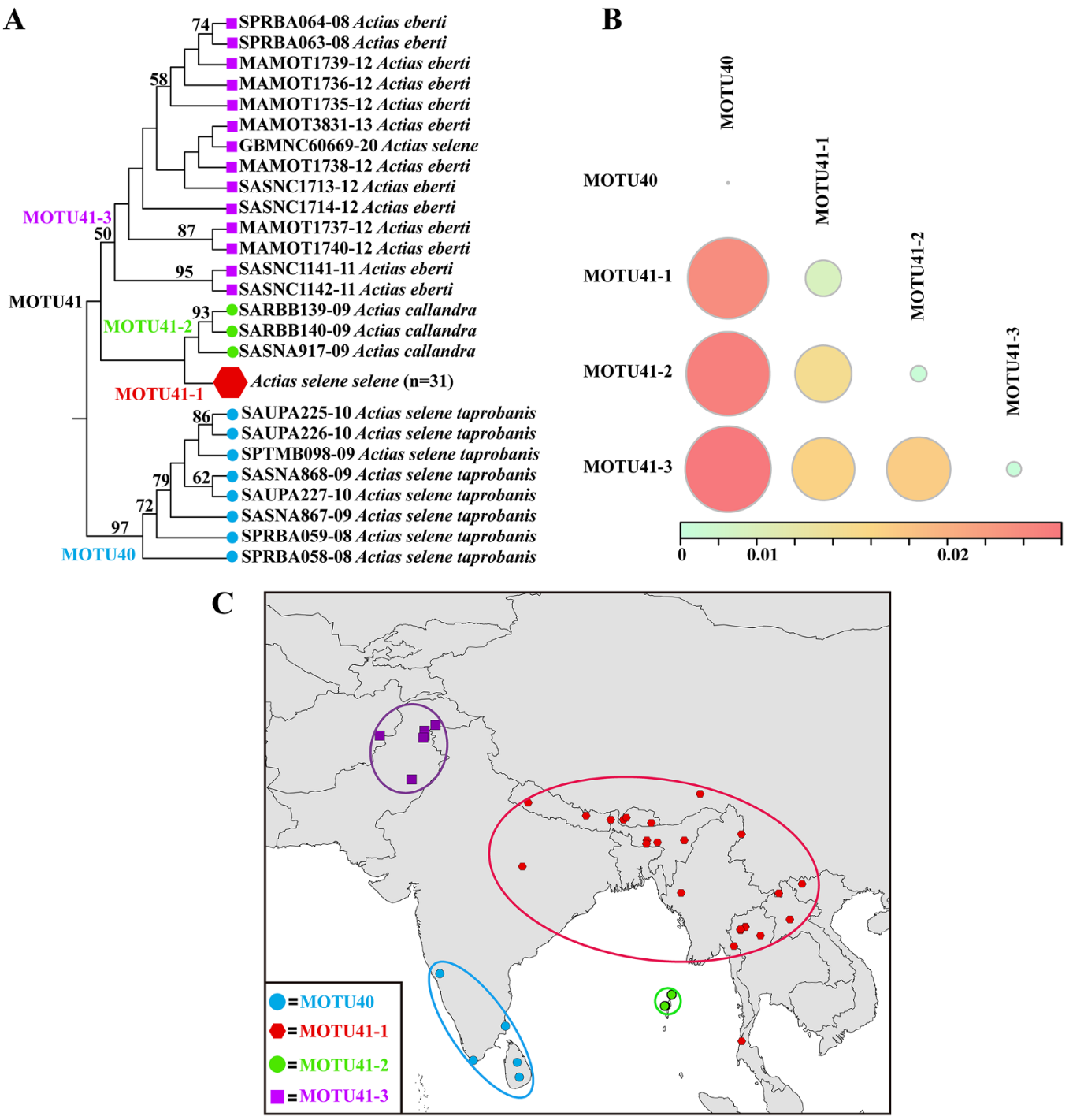


Figure 10. Neighbour-joining tree (A), K2P COI distance (B), and geographical distribution (C) of two species and two subspecies in MOTU40 and MOTU41 (*A. selene*, *A. callandra*, and *A. eberti*).

that differed from its original morphological classification (table S7), indicating the occurrence of misidentification. A representative case is sequence FJ358505 (Pu *et al.*, 2008), which was originally identified morphologically as *A. selene* but clusters within the *A. ningpoana* clade in our phylogeny. It shows minimal genetic divergence from the *A. ningpoana* clade (MOTU39; <1.64%) but high divergence from the *A. selene* clade (MOTU41; >7.08%). Accordingly, the sequences identified as potential misidentifications have been formally reported to the BOLD database management team as evidence-based suggestions for curatorial review, in line with our aim to contribute to the improvement of public data quality.

https://doi.org/10.1017/S0007485326100893 Published online by Cambridge University Press

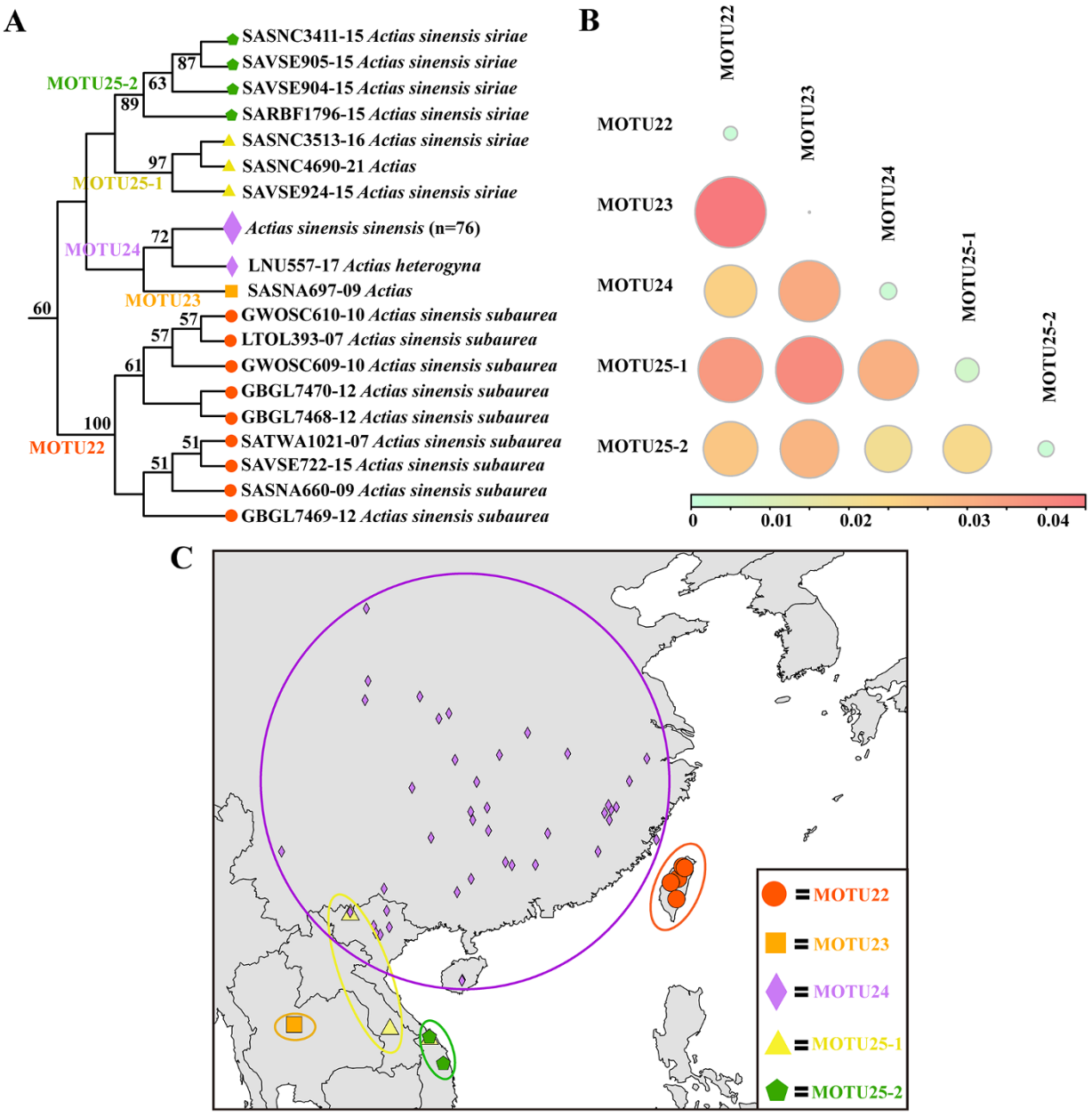


Figure 11. Neighbour-joining tree (A), K2P COI distance (B), and geographical distribution (C) of four species and one subspecies in MOTU22, MOTU23, MOTU24 and MOTU25 (*A. sinensis*).

Species composition and COI identification in Liaoning Province

The application of our global phylogenetic framework provided definitive COI identifications for the historically ambiguous *Actias* fauna of Liaoning Province. All publicly available COI sequences from Liaoning, along with our four newly sequenced specimens from Benxi (BOLD Dataset: https://dx.doi.org/10.5883/DS-CLBX), were placed within the framework with high confidence. This analysis revealed the presence of at least three species in the region: *A. ningpoana*, the *A. artemis/A. dulcinea* complex, and *Actias gnoma* (Butler, 1877). Specifically, three of the four public BOLD sequences from Liaoning and our new Benxi specimens (PV628723 and PV628724) clustered within MOTU36-2, confirming their identity as members of the *A. artemis/A. dulcinea* complex. The previously published sequence FJ358505 (*A. selene*) and the two other newly sequenced specimens from Benxi (PV628729 and PV628734), all from Liaoning Province, were robustly placed within the *A. n. ningpoana* clade (MOTU39-8). The public sequence of *A. gnoma* from Liaoning was correctly placed within its expected clade.

Discussion

Species delimitation in *Actias* is, with 41–55 recognized morphospecies, challenged by morphological ambiguities and the lack of a genus-specific COI threshold standard (Ratnasingham and Hebert, 2007; Huemer *et al.*, 2014; Kitching *et al.*, 2018; Beccaloni *et al.*, 2024). To tackle these challenges, we built a robust framework based on DNA barcoding data, combined with morphological,

https://doi.org/10.1017/S0007485326100893 Published online by Cambridge University Press

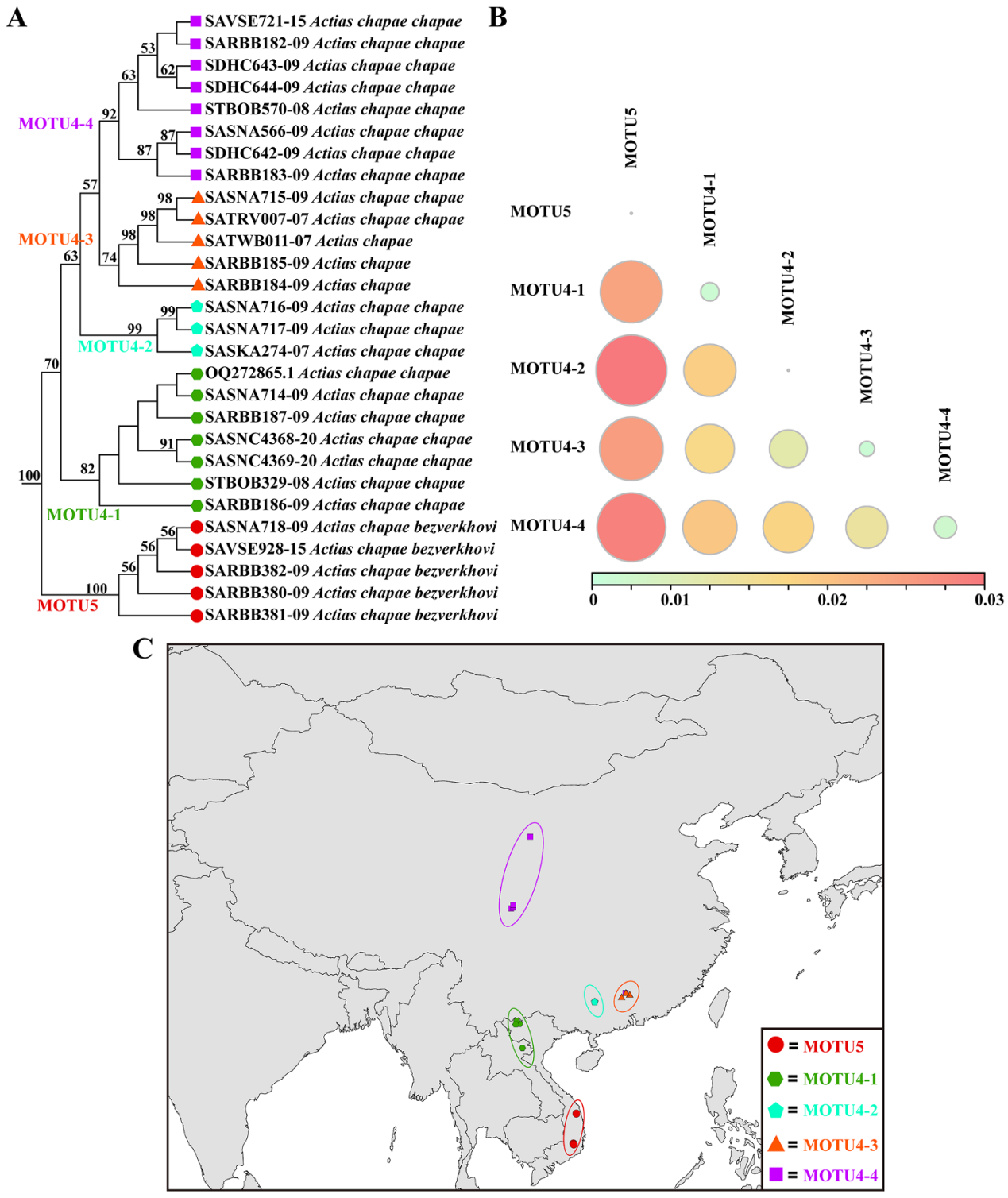


Figure 12. Neighbour-joining tree (A), K2P COI distance (B), and geographical distribution (C) of two species and four subspecies in MOTU4 and MOTU5 (*A. chapae*).

phylogenetic, population genetic (Fst), and biogeographic evidence. A set of 29 MOTUs consistent with morphology-based taxa served as the baseline for determining an *Actias*-specific interspecific K2P COI distance range. The resulting 2.05% threshold that aligns with the established ~2% Lepidopteran benchmark (Hajibabaei *et al.*, 2006; Zahiri *et al.*, 2014) was then applied to resolve species-level taxonomic uncertainties across the genus. This approach not only delineated 15 additional MOTUs from previously ambiguous assignments but was also key to resolving long-standing ambiguities in sequence identity. The species-level threshold (2.05%) provided a consistent criterion for delimitation, consequently supporting the elevation of morphologically defined subspecies to species status where genetic distances warranted (MOTU5, MOTU22, MOTU25, MOTU42, and

https://doi.org/10.1017/S0007485326100893 Published online by Cambridge University Press

MOTU40). By applying the empirically derived subspecific threshold range (1.00–2.05%), we were able to validate robust subspecies hypotheses and, conversely, to flag taxonomic units that lack coherent support, thereby identifying priority cases for future taxonomic revision. The infraspecific threshold consolidated synonyms (MOTU44) and, conversely, identified divergent intraspecific lineages (e.g. *A. n. ningpoana* (MOTU39-4, 5, 6, 7, and 8). Our work establishes a replicable, evidence-based system for generating taxonomic hypotheses in *Actias*.

Our analysis, applying the integrative framework established above, provides new evidence to address several taxonomic debates stemming from conflicting historical classifications. For instance, while *Actias bulbosa* Nässig & Treadaway, 1997 is variably elevated to species rank (BOLD) or as a subspecies of *Actias philippinica* Nässig & Treadaway, 1997 (Kitching *et al.*, 2018), our genetic data support its recognition as a distinct species, as its divergence exceeds our empirical interspecific threshold. Conversely, for *A. diana* (often equated with *A. maenas diana*), our data support its subspecific status within *A. maenas*, consistent with its classification in Kitching *et al.* (2018).

Likewise, the taxonomic complex comprising *Actias acutapex* Kishida, 2000, *Actias sumbawaensis* Paukstadt, Paukstadt & Rougerie, 2010, and *Actias timorensis* Paukstadt, Paukstadt & Rougerie, 2010, which are treated as subspecies of *Actias groenendaeli* Roepke, 1954 in some classifications (e.g. Wikipedia: accessed on 4 March 2025; Kitching *et al.*, 2018) but as full species in BOLD, is evaluated by our data. Their pairwise genetic distances fall within the range of interspecific variation for *Actias*, and their phylogenetic separation lead us to support their recognition as distinct species, consistent with their treatment in BOLD.

A particularly instructive case is *A. xenia*, which was originally described as a subspecies of *A. artemis* before being elevated to species level (Kitching *et al.*, 2018; Coppens, 2019). Our data show that while it forms a distinct, allopatric subclade, it exhibits a low genetic distance of 1.08% from *A. artemis*, a value below our *Actias*-specific interspecific threshold of 2.05%. Therefore, based on our calibrated criteria, we support its classification at the subspecific level, i.e. as *A. artemis xenia*. This case, however, also precisely underscores a limitation of the single-gene approach. Our framework could not resolve the distinction between *A. artemis* and *A. dulcinea*, which show minimal genetic divergence and broadly overlapping distributions. This pattern suggests underlying evolutionary complexity that cannot be resolved here, pinpointing a key question requiring phylogenomic data for clarification. Collectively, these applications showcase the framework's capacity to generate specific, testable hypotheses for resolving taxonomic ambiguities, while precisely demarcating the boundaries of its current analytical scope.

Building on the specific cases and limitations discussed above, this study establishes a robust framework for *Actias* taxonomy while clarifying key avenues for future research. Firstly, our conclusions are based primarily on the COI barcode region. Although this marker is highly effective for initial species delimitation, it may be insufficient to fully resolve recent radiations or complex phylogenetic relationships where incomplete lineage sorting or introgression is involved. Thus, future studies incorporating genome-scale data (e.g. ultra-conserved elements or whole genomes) will be crucial for elucidating these difficult nodes. Secondly, while our taxonomic inferences are grounded in quantitative evidence, they are sometimes constrained by data availability. For example, the proposed synonymization of *A. heterogyna* is based on a single sequence, and the phylogenetic position of *A. witti* remains unstable due to its short sequence length (506 bp). These specific cases highlight the need for targeted sampling from type localities and the generation of full-length barcodes to conclusively test our hypotheses. Finally, beyond taxonomy, our biogeographic analysis reveals that the European and American species are phylogenetically nested within Asian clades. This pattern presents a compelling evolutionary puzzle regarding their historical biogeography. However, the limited resolution of a single gene fragment precludes detailed inference into the timing and mechanisms of these transcontinental distributions. Therefore, our framework establishes the necessary phylogenetic foundation for future studies to address these macroevolutionary questions directly, using phylogenomic and biogeographic modelling approaches.

Supplementary material. The supplementary material for this article can be found at https://doi.org/10.1017/S0007485326100893.

Acknowledgements. This work was supported by the National Natural Science Foundation of China (grant no: 31972617), the Applied Basic Research Program of Liaoning Province (grant no: 2022JH2/101300178), and the China Agriculture Research System (CARS-18).

Competing interests. The authors declare that no potential conflicts of interest exist.

References

Aguila RN, Plasencia EO, Maravi PF and Wahlberg N (2012) Cuban *Calisto* (Lepidoptera, Nymphalidae, Satyrinae), a review based on morphological and DNA data. *Zookeys* **165**, 57–105. https://doi.org/10.3897/zookeys.165.2206

Albertoni FF and Duarte M (2015) Immature stages of *Adeloneivaia fallax* (Lepidoptera: Saturniidae). *Florida Entomologist* **98**, 178–185. https://doi.org/10.1653/024.098.0131

Alex Smith M, Fernández-Triana JL, Eveleigh E, Gómez J, Guclu C, Hallwachs W, Hebert PD, Hrcek J, Huber JT, Janzen D, Mason PG, Miller S, Quicke DL, Rodriguez JJ, Rougerie R, Shaw MR, Várkonyi G, Ward DF, Whitfield JB and Zaldívar-Riverón A (2013) DNA barcoding and the taxonomy of *Microgastrinae wasps* (Hymenoptera, Braconidae): impacts after 8 years and nearly 20 000 sequences. *Molecular Ecology Resources* **13**, 168–176. https://doi.org/10.1111/1755-0998.12038

Beccaloni G, Scoble M, Kitching I, Simonsen T, Robinson G, Pitkin B, Hine A, Lyal C, Ollerenshaw J, Wing P and Hobern D (2024) Global Lepidoptera Index (version 1.1.24.335). In Bánki O, Roskov Y, Döring M, Ower G, Hernández Robles DR, Plata Corredor CA, Stjernegaard Jeppesen T, Örn A, Pape T, Hobern D, Garnett S, Little H, DeWalt RE, Ma K, Miller J, Orrell T, Aalbu R, Abbott J, Aedo C, et al. (eds.), *Catalogue of Life (Version 2024-12-19)*. Amsterdam, Netherlands: Catalogue of Life. https://doi.org/10.48580/dglq4-49xk

Collins MM and Weast RD (1961) *Wild Silk Moths of the United States: Saturniinae*. Cedar Rapids, IA: Collins Radio Company.

Coppens B (2019) Written by Bart Coppens; based on a real life breeding experience. https://breedingbutterflies.com/actias-dulcinae-sweetheart-moonmoth/ (accessed 4 March 2025).

De Biaggi M, Leccia MF, Kroupa A and Monje JC (2010) Creating a biodiversity inventory in protected areas to increase knowledge of their natural heritage and to improve land management. *Journal on Protected Mountain Areas Research and Management* **2**, 49–52. https://doi.org/10.1553/eco.mont-2-1s49

ESRI (2020) ArcGIS Desktop: Release 10.8.1. Redlands: Environmental Systems Research Institute. https://www.scirp.org/reference/referencespapers?referenceid=3235216 (accessed 4 March 2025).

Excoffier L and Lischer HE (2010) Arlequin suite ver 3.5: a new series of programs to perform population genetics analyses under Linux and Windows. *Molecular Ecology Resources* **10**, 564–567. https://doi.org/10.1111/j.1755-0998.2010.02847.x

García-Souto D, Zumalave S, Martínez-Romero JM, Marí-Mena N, Vizcaíno A and Vila M (2025) Phylomitogenomics supports *Actias isabellae* (Graells, 1849) as the definitive scientific name of the Spanish moon moth (Lepidoptera, Saturniidae). *Genetica* **153**, 15. https://doi.org/10.1007/s10709-025-00231-w

GBIF Secretariat (2023) GBIF backbone taxonomy. Checklist dataset https://doi.org/10.15468/39omei accessed via GBIF.org on 2025-11-05.

Guo YJ, An SQ, Fang ZG, Wei SF, Shen ZH, Chen ZY and He ZQ (2024) A taxonomic revision of the genus *Goniogryllus* in China (Orthoptera: Gryllidae: *Gryllinae*). *Arthropod Systematics & Phylogeny* **82**, 567–584. https://doi.org/10.3897/asp.82.e108699

Hajibabaei M, Janzen DH, Burns JM, Hallwachs W and Hebert PDN (2006) DNA barcodes distinguish species of tropical Lepidoptera. *Proceedings of the National Academy of Sciences of the USA* **103**, 968–971. https://doi.org/10.1073/pnas.0510466103

Hebert PDN, Cywinska A, Ball SL and deWaard JR (2003) Biological identifications through DNA barcodes. *Proceedings of the Royal Society B* **270**, 313–321. https://doi.org/10.1098/rspb.2002.2218

Hebert PDN, Dewaard JR and Landry JF (2010) DNA barcodes for 1/1000 of the animal kingdom. *Biology Letters* **6**, 359–362. https://doi.org/10.1098/rsbl.2009.0848

Hodges RW (2005) Order Lepidoptera: butterflies and moths. In Triplehorn CA and Johnson NF (eds.), *Borror and Delong's Introduction to the Study of Insects*, 7th Edn. Cole, Belmont: Thomson Brooks, pp. 571–647.

Huemer P, Mutanen M, Sefc KM and Hebert PDN (2014) Testing DNA barcode performance in 1000 species of European Lepidoptera: large geographic distances have small genetic impacts. *PLoS ONE* **9**, e115774. https://doi.org/10.1371/journal.pone.0115774

Ichter J, Leccia MF, Touroult J, Blandin P, Aberlenc HP, Holtof JF, Foret J, Bonet R, Pascal O, Dusoulier F, Gargominy O and Poncet L (2010) Les inventaires généraux de la biodiversité en France et dans Le Monde. In *Revue des All Taxa Biodiversity Inventories*. Paris, France: UMS. PatriNat/Parc national du Mercantour, 51p, Available at: http://www.patrinat.fr/sites/patrinat/files/atoms/files/2018/11/patrinat_2018_-_108_-_ichter_et_al_2018_les_inventaires_generaux_de_la_biodiversite_atbi.pdf (accessed 2 January 2023).

Katoh K, Rozewicki J and Yamada KD (2017) MAFFT online service: multiple sequence alignment, interactive sequence choice and visualization. *Briefings in Bioinformatics* **20**, 1160–1166. https://doi.org/10.1093/bib/bbx108

Kitching IJ, Rougerie R, Zwick A, Hamilton CA, St Laurent RA, Naumann S, Ballesteros Mejia L and Kawahara AY (2018) A global checklist of the Bombycoidea (Insecta: Lepidoptera). *Biodiversity Data Journal* **12**, e22236. https://doi.org/10.3897/BDJ.6.e22236

Liu QN, Zhu BJ, Dai LS, Wei GQ and Liu CL (2012) The complete mitochondrial genome of the wild silkworm moth, *Actias selene*. *Gene* **505**, 291–299. https://doi.org/10.1016/j.gene.2012.06.003

Markee A, Godfrey RK, Frandsen PB, Weng YM, Triant DA and Kawahara AY (2024) De novo long-read genome assembly and annotation of the luna moth (*Actias luna*) fully resolves repeat-rich Silk genes. *Genome Biology and Evolution* **16**, evae148. https://doi.org/10.1093/gbe/evae148

Nässig WA and Peigler RS (1984) The life-history of *Actias maenas* (Saturniidae). *Journal of the Lepidopterists' Society* **38**, 114–123.

Núñez R, Genaro JA, Miller J, Barro-Cañamero A, Álvarez Y, Fernández DM, Minno MC, Turner T, Turlan V, Wahlberg N, Pérez-Asso AR and Hausmann A (2023) DNA barcodes of the greater antillean butterflies (Lepidoptera: Papilionoidea) suggest a richer, more isolated fauna and higher endemism. *Biological Journal of the Linnean Society* **140**, 447–458. https://doi.org/10.1093/biolinnean/blad015

Núñez R, Genaro JA, Pérez-Asso A, Murillo-Ramos L, Janzen DH, Hallwachs W, Wahlberg N and Hausmann A (2020) Species delimitation and evolutionary relationships among *Phoebis* New World sulphur butterflies (Lepidoptera, Pieridae, Coliadinae). *Systematic Entomology* **45**, 481–492. https://doi.org/10.1111/syen.12408

Park JS, Kim MJ and Kim I (2016) The complete mitochondrial genome of the moon moth, *Actias aliena* (Lepidoptera: Saturniidae). *Mitochondrial DNA Part A* **27**, 149–150. https://doi.org/10.3109/19401736.2013.878918

Pu JM, Wu S, Huo XM, Wang H, Xia RX, Li XS, Wang ZD, Luo CB and Liu YQ (2008) DNA barcode and phylogenetic analysis of the moon silkworm, *Actias selene*. *Acta Sericologica Sinica* **35**(1), 154–159 (in Chinese). https://doi.org/10.3969/j.issn.0257-4799.2009.01.027

Puillandre N, Brouillet S and Achaz G (2021) ASAP: assemble species by automatic partitioning. *Molecular Ecology Resources* **21**, 609–620. https://doi.org/10.1111/1755-0998.13281

Puillandre N, Lambert A, Brouillet S and Achaz G (2012) ABGD, Automatic Barcode Gap Discovery for primary species delimitation. *Molecular Ecology* **21**, 1864–1877. https://doi.org/10.1111/j.1365-294X.2011.05239.x

Ratnasingham S and Hebert PDN (2007) BOLD: the barcode of life data system (http://www.barcodinglife.org). *Molecular Ecology Notes* **7**, 355–364. https://doi.org/10.1111/j.1471-8286.2007.01678.x

Rozas J, Ferrer-Mata A, Sánchez-delbarrio JC, Guirao-Rico S, Librado P, Ramos-Onsins SE and Sánchez-Gracia A (2017) DnaSP 6: DNA sequence polymorphism analysis of large data sets. *Molecular Biology and Evolution* **34**, 3299–3302. https://doi.org/10.1093/molbev/msx248

Schattanek-Wiesmair B, Huemer P, Wieser C, Stark W, Hausmann A, Koblmüller S and Sefc KM (2024) A DNA barcode library of Austrian Geometridae (Lepidoptera) reveals high potential for DNA-based species identification. *PLoS ONE* **19**, e0298025. https://doi.org/10.1371/journal.pone.0298025

Schmidt S, Schmid-Egger C, Morinière J, Haszprunar G and Hebert PD (2015) DNA barcoding largely supports 250 years of classical taxonomy: identifications for Central European bees (Hymenoptera, *Apoidea partim*). *Molecular Ecology Resources* **15**, 985–1000. https://doi.org/10.1111/1755-0998.12363

Sheth BP and Thaker VS (2017) DNA barcoding and traditional taxonomy: an integrated approach for biodiversity conservation. *Genome* **60**, 618–628. https://doi.org/10.1139/gen-2015-0167

Simon C, Buckley TR, Frati F, Stewart JB and Beckenbach AT (2006) Incorporating molecular evolution into phylogenetic analysis, and a new compilation of conserved polymerase chain reaction primers for animal mitochondrial DNA. *Annual Review of Ecology, Evolution, and Systematics* **37**, 545–579. https://doi.org/10.1146/annurev.ecolsys.37.091305.110018

Tamura K, Stecher G and Kumar S (2021) MEGA11: molecular evolutionary genetics analysis version 11. *Molecular Biology and Evolution* **38**, 3022–3027. https://doi.org/10.1093/molbev/msab120

Triant DA and Pirro S (2023) The complete genome sequence of *Actias luna* (Saturniidae, Lepidoptera), the luna moth. *Biodiversity Genomes* **2023**, 10-56179. https://doi.org/10.56179/001c.75356

Tsai CL, Wan X and Yeh WB (2014) Differentiation in stag beetles, *Neolucanus swinhoei* complex (Coleoptera: Lucanidae): four major lineages caused by periodical Pleistocene glaciations and separation by a mountain range. *Molecular Phylogenetics & Evolution* **78**, 245–259. https://doi.org/10.1016/j.ympev.2014.05.004

Wagner DL (2005) *Caterpillars of Eastern North America: a guide to identification and natural history*. Princeton, New Jersey: Princeton University Press.

Wang Y, Zhou ZY, Lu C, Xiang ZH, Yang B and Zeng HM (1997) DNA extraction from single egg of silkworm. *Journal of Southwest Agricultural University* **19**, 434–437. in Chinese.

Wu Y and Naumann S (2006) The preimaginal instars of *Actias chapae* (MELL, 1950) (Lepidoptera: Saturniidae). *Nachrichten Des Entomologischen Vereins Apollo* **27**, 17–21.

Zahiri R, Lafontaine JD, Schmidt BC, Dewaard JR, Zakharov EV and Hebert PD (2014) A transcontinental challenge-a test of DNA barcode performance for 1,541 species of Canadian Noctuoidea (Lepidoptera). *PLoS ONE* **9**, e92797. https://doi.org/10.1371/journal.pone.0092797

Zborowski P and Edwards T (2007) *A Guide to Australian Moths*. Collingwood: CSIRO Publishing.

Zhang J, Cong Q, Shen J, Opler PA and Grishin NV (2021) Genomics-guided refinement of butterfly taxonomy. *The Taxonomic Report* **9**, 1–55.

Zhang J, Kapli P, Pavlidis P and Stamatakis A (2013) A general species delimitation method with applications to phylogenetic placements. *Bioinformatics* **29**, 2869–2876. https://doi.org/10.1093/bioinformatics/btt499

https://doi.org/10.1017/S0007485326100893 Published online by Cambridge University Press

Zhang YJ, Fang H and Jiang L (2022) Comparative morphology of the larval mouthparts among three *Actias* (Lepidoptera: Saturniidae), with descriptions on atypical spinnerets. *Zoomorphology* **141**, 173–181. https://doi.org/10.1007/s00435-022-00555-7

Zhao F, Su TJ, He B, Jiang K, Zuo CX, Lin GH and Huang ZH (2021) Complete mitochondrial genome of *Actias dubernardi* (Lepidoptera: Saturniidae). *Mitochondrial DNA Part B* **6**, 627–628. https://doi.org/10.1080/23802359.2021.1875929

Zhong M (2016) Quantifying wing shape and size of saturniid moths with geometric morphometrics. *The Journal of the Lepidopterists' Society* **70**, 99–107. https://doi.org/10.18473/lepi.70i2.a4

https://doi.org/10.1017/S0007485326100893 Published online by Cambridge University Press